Experimental observation of phase transformation front of SMA under impact loading

He Huang[1], Dominique Saletti[2], Stephane Pattofatto[1], Feifei Shi[1,4], Han Zhao[1,*]

[1] LMT-Cachan, ENS Cachan/CNRS 8535/UPMC, 61 Avenue du president Wilson, 94235 Cachan cedex, France
[2] Laboratoire de Biomécanique, Arts et Métiers ParisTech, 151, boulevard de l'Hôpital,75013 Paris, France
[3] School of Aeronautics, Northwestern Polytechnical university, 710072 Xi'an, China
* Corresponding author: zhao@lmt.ens-cachan.fr

Abstract Pseudoelasticity is one of the main characteristics of shape memory alloys (SMAs), allowing them to recover their initial state after undergoing large deformation. This is due to the martensitictransformation (MT) occurring in the material, turning the austenitic phase into a stress-induced martensitic phase when a mechanical load is experienced. Even if such an effect was largely studied in the past decades under quasi-static loading, the dependence of this effect of the loading rates was rather poorly documented. Only some studies have reported the strain rate dependence of the macroscopic behaviour of SMAs, but no detailed observation of the transformation process under impact loading is available.
This paper investigates the influence of the loading rate applied to a NiTi SMA at the level of the MT, providing experimental data of not only the macroscopic stress-strain curves, but also the corresponding observation of the heterogeneous strain field during the test. Main testing results are obtained under tensile loading. Experiments were conducted at three different levels of prescribed velocity : 0.01 mm/s, 1 mm/s and 5000 mm/s, using a classical loading machine for the quasi-static cases and a Split Hopkinson Tensile Bar (SHTB) for the dynamic cases. The observations of the heterogeneous strain field during the tests were made using a digital image correlation (DIC). Additional results under double shear test at various loading rate will be also presented.

Keywords Impact testing, Phase transition; NiTi shape memory alloy; Domain patterns and domain spacing; Strain rate.

1. Introduction

Shape memory alloys (SMA) have a great potential of applications in a lot of innovative technologies owing to two specific properties: the shape memory effect and pseudoelasticity [1]. In particular, NiTi-based SMA are widely used as biomaterials (to manufacture heart artery stents for instance) or in mechanical applications such as actuators, smart materials in the automotive industry, household appliances, and so on. The ability of NiTi alloys to undergo large strains is due to the transformation, under mechanical loading, of initial austenite to stress-induced martensite (SIM). This specific stress-induced martensitic transformation is associated to a mechanism of propagation of bands into the specimen as in localization phenomena (Luders bands, Portevin-Le Chatelier effect [2], compaction of foams ([3-4]), which leads to a non-homogeneous strain state ([5-7]).
Technically, the observation of the bands and the influence of strain rate on the propagation of the martensitic transformation has been initiated fifteen years ago ([6-8]). New measuring techniques, such as Digitial Image Correlation (DIC) that catches the measurable difference of strain between elastically loaded austenite and mechanically transformed martensite([9-10]), as well as the Infrared thermography (IRT) that takes advantage of the fact that the transformation of austenite into martensite is exothermic ([11-12]), have been used in the last decade. In the open literature, particular results are reported about the nucleation sites and the number of bands ([13]), the propagation of the transformation front, or the effect of stress concentration ([14]).

Under higher strain rates (more than 10 /s), some authors have studied the strain rate sensitivity of NiTi in compression ([15-19]) with Split Hopkinson Pressure Bars (SHPB), a system commonly used for accurate measurement of dynamic and macroscopic stress-strain responses of materials

([20-21]). It appears that SIM transformation is rate-dependent so that the stress triggering the transformation process increases with strain rate. There are also a few papers that present some experimental results with tensile Hopkinson bar tests (strain rate up to 1.67 /s in[22] and up to 1200 /s in [15]). Unfortunately, all these results under impact loading rate are only based on macroscopic measurements which are the nominal strain or stress. The observation of the transforming regions of NiTi alloys is not yet reported, probably due to the experimental difficulty to get these results at such strain rates. Thus, the description of nucleation sites, number of bands, transformation front velocity under higher strain rate are almost unknown. There is no available shear testing results under impact loading.

The present work wishes to provide a measurement of NiTi SMA behavior under tensile as well as shear loading up to an intermediate strain rate regime around 100 /s (3 decades higher than previous studies). In addition, heterogenous strain fields due to transforming regions is measured, coupled with a tensile Hopkinson bar system. For this purpose, strain fields of the sample are measured by Digital Image Correlation procedures using pictures captured with a high speed camera.

2. Experimental setup and macroscopic results

2.1 Tensile tests

2.1.1 NiTi specimens and quasi-static tests

The material of this study is taken from NiTi polycristalline cold-rolling sheets, in the cold-rolling direction. The metallurgical composition is 50.7 wt.% Ni and 49.3 wt.% Ti ([23]). All the experiments are performed at room temperature, clearly above the characteristic temperature A_f so that for stress-free condition the specimen is in a full austenite state. A single plate specimen, dog bone shaped, as schematically presented in the upper left corner of figure 1, is used for all the experiments. In its central part, the specimen is 60 mm long, 2.6 mm wide and 0.5 mm thick.

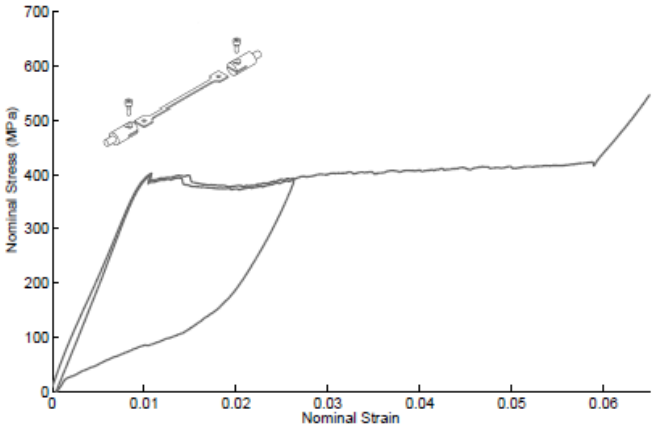

Fig. 1: Static strain-stress curve for a prescribed velocity of 0.01 mm/s ($1.4x10^{-4}$ /s), at room temperature

For the fixation in the grips, the width is 10 mm so that the fillet radius of 10 mm leads to a stress concentration. It is observed that this triggers the SIM transformation at both ends of the central part of the specimen. This is acceptable because the paper is focused on propagation of the transformation, not on its nucleation. For all the experiments, the specimen is fixed between two

tabs that can further be screwed (i) in the bars for dynamic tensile experiment, (ii) in a clamping system for static experiments. This allows to be more confident in the comparison of experimental results obtained with different devices. We could ensure that there is no sliding of the specimen during monotonic static or dynamic tension experiments due to the presence of a screw that fits into one hole machined into each end of the specimen. Quasi-static tensile tests were performed on an electromechanical Instron device so there was no heating of the specimen through the gripping system. Experiments were done at two different prescribed velocities : 0.01 mm/s ($1.4x\ 10^{-4}$/s) and 1 mm/s ($1.4x\ 10^{-2}$/s). Each experiment was repeated twice in order to check repeatability of the measurements. The nominal stress-strain curve obtained at 0.01 mm/s is shown in figure 1.
Three domains appear on the curve. First the elastic tension of the initial austenite phase for strains up to 0.01. Then the stress plateau associated to the pseudoelastic domain of interest in this study begins. It corresponds to the stress-induced martensitic (SIM) transformation for strains up to 0.06. One unloading-reloading cycle has been performed in the pseudoelastic domain in order to show that the reverse transformation is effectively reversible. It can be noticed that two serrations are visible at the beginning of the pseudoelastic domain. This phenomenon is due to the heterogeneity of the martensitic transformation ([12]). At a third stage, the supposed "fully" martensitic specimen is submitted to elastic tension. The vocabulary "fully martensitic" refers in fact to the end of the SIM transformation process even if it has been documented that probably all austenite has not been transformed yet ([24]). In this experiment, maximal strain is under 0.08 and there is no evidence of plastic deformation during tension.

2.1.2 The tensile Hopkinson bar experiment

The use of Hopkinson bars as a measurement technique has been introduced at the end of the 19th century and has led to many developments in the field of analysis of material behaviour under dynamic loading ([20], [25]). Hopkinson bar measurement allows to obtain an accurate measurement of dynamic forces and velocities at both ends of the specimen. The device used in this study is a Split Hopkinson Tensile Bar (SHTB) as schematized in figure 2. The apparatus is composed of two bars of 10 mm diameter, called the input and the output bars, made of maraging steel. The specimen (equipped with its end tabs) is tightly screwed at the end of each bar. The tabs are manufactured in the same material as the bars and designed so as to minimize any mass effect by matching the same acoustic impedance as the bars. The loading principle is the following: first a tensile elastic energy is stored in the input bar along a length L between points A and B of the input bar, then this energy is suddenly released from point B so that an incident tension pulse reaches the specimen ([26]). The initial elastic energy controls the subsequent strain and strain rate applied to the specimen. The initial load N_0 is applied with a hydraulic jack, and, to perform a test at an initial velocity of around 1000 mm/s, an initial load of around 5 kN is applied.

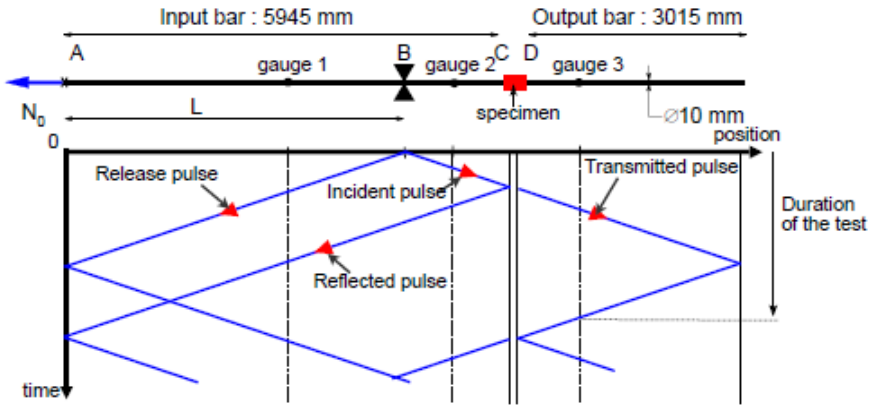

Fig. 2: Split Hopkinson Tensile Bar dimensions and corresponding lagrange diagram.

A significant increase of stress level is observed with impact strain rate, as shown in Figure 3.

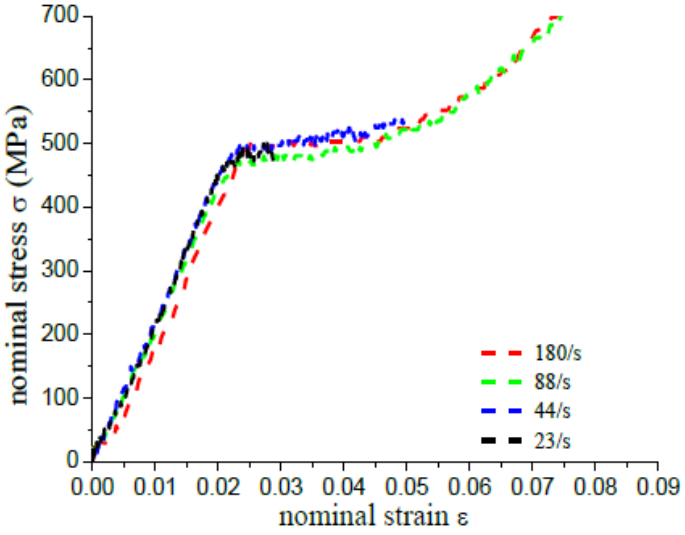

Figure 3 Stress strain curves at intermediate strain rates

2.2. Shear tests

Double shearing test can be realized which might prevent from geometrical instabilities. Divers versions of this test had been developed in the past decades [27-29]. A modified double shearing device to better fit with the 60mm-diameter Split Hopkinson pressure bar was developed by Merle [30]. Figure 4 shows the clamping device and specimen for the shearing tests. The specimen has two symmetric shearing zones of 3mm width and 20mm length. The clamping device is composed of the two moving coaxial pieces.

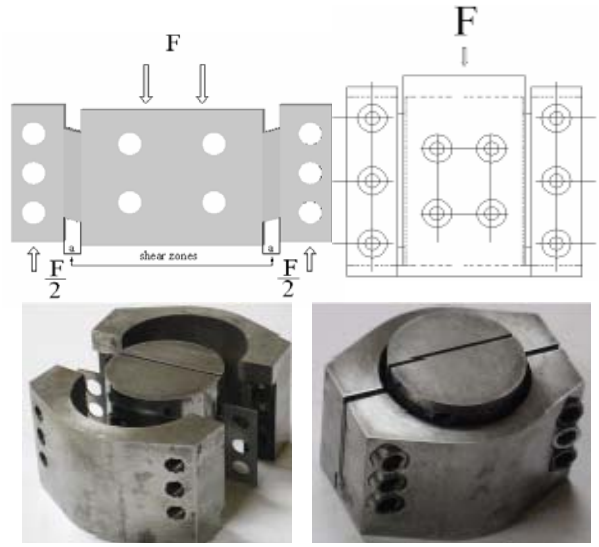

Fig. 4 Double shear specimen and shear device

Quasi-static tests were performed using a classical hydraulic testing machine with the device mentioned above. Dynamic tests were performed using the split Hopkinson of aluminum bars with a diameter of 60mm with 4m long incident bar and 2.5m long transmitted bar. The schematic drawing of the bars is shown in figure 5.

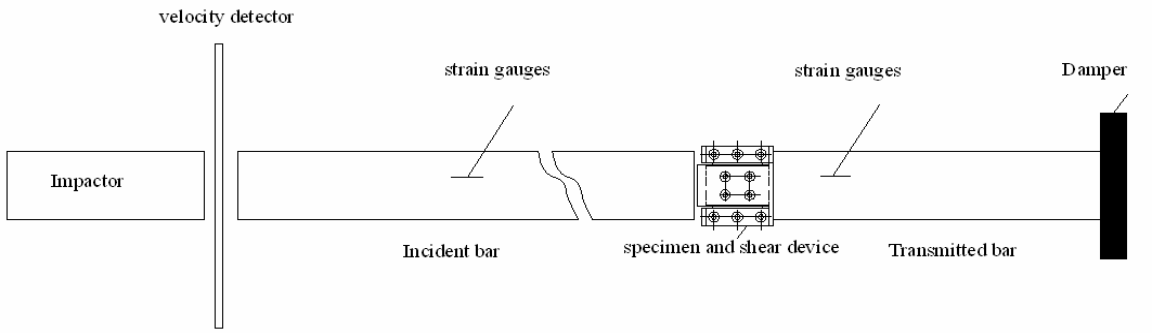

Fig.5 Schematic drawing of 60mm aluminum Hopkinson bar and device

Based on the plane shear assumption, the equivalent strain is calculated with measured displacement between the two clamping pieces d (Eqn 1.) and equivalent stress with the force F (Eqn 2).

$$\varepsilon_{eq} = \frac{\mathrm{d}}{l\sqrt{3}} \tag{1}$$

$$\sigma_{eq} = \tau\sqrt{3}\,,\ \tau = \frac{F}{S}. \tag{2}$$

Figure 6 shows first results at various strain rate. The same tendency of stress increases is also

observed.

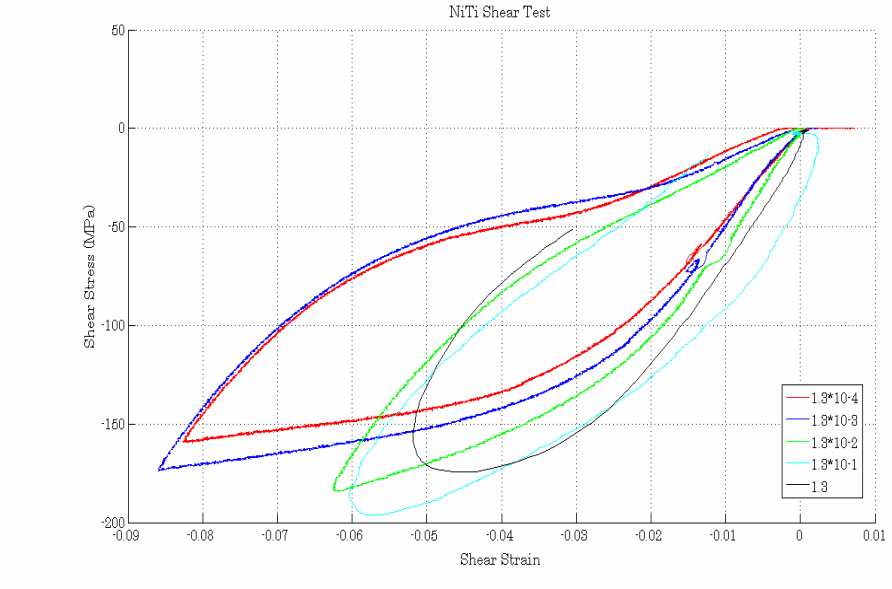

Figure 6 Shear stress-strain curves at various strain rates

3. Measurement of strain fields

3.1 Digital Image Correlation (DIC) setup

To acquire images, different devices were used, depending of the performed test. For low frequency acquisition, a reflex camera (Canon EOS) was used and for high frequency acquisition, fast cameras (PHOTRON) were used. The main difference between the two ways to get pictures is that for fast camera, the resolution is lower than for reflex camera. Subsequently, the spatial resolution is poorer for dynamic tests: the resolution of the fast camera is in inverse proportion to frame rate even if, for the last test, a more efficient camera was used in comparison with the previous test. This impact directly the accuracy of the optical measurement. In order to allow DIC computations, a speckle was applied on the observed surface of the specimen with black and white paint. Moreover, in order to avoid heating of the specimen surface, the lighting was done with LED lights during the quasi-static experiments and with short time light exposition of the specimen during the dynamic experiments. The principle of the used DIC computation program (CorreliQ4) is given in [31-32]. A first analysis of DIC results allows to give qualitative information on the phenomena taking place during the tests. Basic observation on figure 7, resulting from a quasi-static tensile test at 0.01 mm/s, shows that only two admissible strains are visible: a 1 % strain zone (supposed to be the austenitic phase) and a 6 % strain zone (supposed to be the stress-induced martensitic phase). An enlargement of the SIM region during the test can be observed.

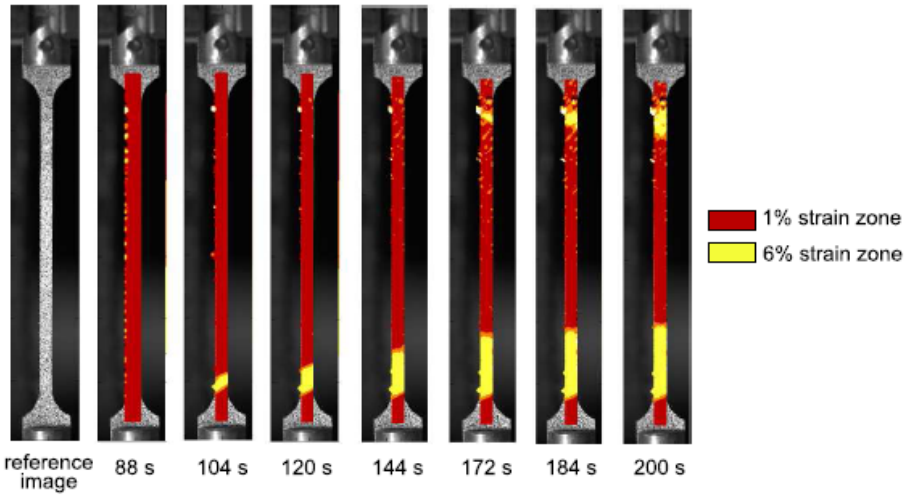

Fig. 7: Strain maps for quasi-static tensile test performed at 0.01 mm/s

The same image analysis can be also applied to the double shear tests. Figure 8 shows a strain map of shear tests. In contrast with tensile test, a rather homogeneous strain field was observed.

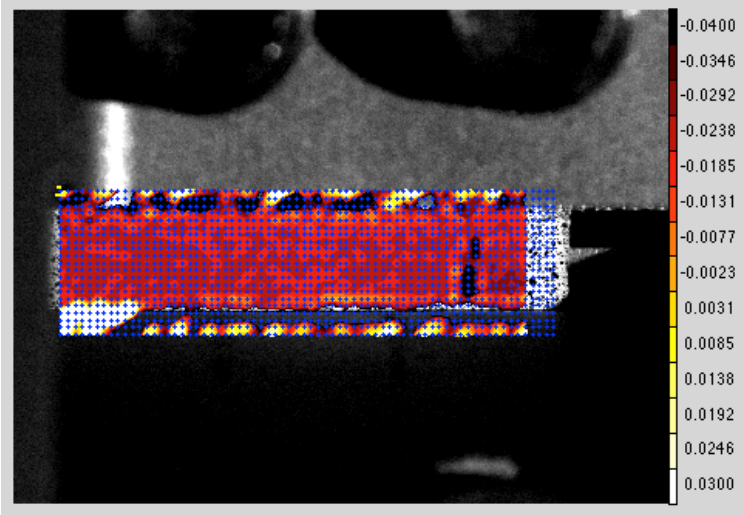

Figure 8, strain field measurement during shear tests

4 Conclusions

This paper used Split Hopkinson pressure bar system and high-speed testing machine to investigate the pseudoelastic deformation of a NiTi plate specimen at various strain rates. It provides original results of the strain rate dependence under not only tensile but shear loadings. In addition, the image analysis were used in all the testing which allows a measurement of strain fields.

Acknowledgements

Authors would like to express their thanks to the research team led by Prof. Sun Qingping of Hong Kong University of Science and Technology for his advice and supply of specimen used in all our experiments.

References

[1] Lagoudas D., Shape Memory Alloys, Springer (2008)
[2] Benallal A, Berstad T, Borvik T, Hopperstad OS, Nogueira de Codes R (2008) Effects of strain rates on the characteristics of PLC deformation bands for AA5083-H116 aluminium alloy. Philosophical Magazine 88(28)(29):3311-3338.
[3] El nasri I, Pattofatto S, Zhao H, Tsitsiris H, Hild F, Girard Y (2007) Shock enhancement of cellular stuctures under impact loading : Part I Experiments. Journal of the Mechanics and Physics of Solids 55:2652-2671.
[4] Pattofatto S, El Nasri I, Zhao H, Tsitsiris H, Hild F, Girard Y (2007) Shock enhancement of cellular stuctures under impact loading : Part II analysis. Journal of the Mechanics and Physics of Solids 55:2672-2686.
[5] Feng P and Sun QP (2006) Experimental investigation on macroscopic domain formation and evolution in polycrystalline NiTi microtubing under mechanical force. Journal of the Mechanics and Physics of Solids 54:1568-1603.
[6] Shaw JA and Kyriakides S (1998) Initiation and propagation of localized deformation in elasto-plastic strips under uniaxialtension. International Journal of Plasticity 13(10):837-871.
[7] Taillard K, Arbab Chirani S, Calloch S, Lexcellent C (2008) Equivalent transformation strain and its relation with martensite volume fraction for isotropic and anisotropic shape memory alloys. Mechanics of Materials 40:151-170.
[8] Shaw JA and Kyriakides S (1995) Thermomechanical aspects of NiTi. Journal of the Mechanics and Physics of Solids 43(8):1243-1281.
[9] Murasawa G, Yoneyama S, Sakuma T, TakashiM(2006) Influence of Cyclic Loading on Inhomogeneous Deformation Behavior Arising in NiTi Shape Memory Alloy Plate. Materials Transactions 47(3):1-7.
[10] Daly S, Ravichandran G, Bhattacharya K (2007) Stress-induced martensitic phase transformation in thin sheets of Nitinol. Acta Materialia 55:3593-3600.
[11] Pieczyska EA, Gadaj SP, Nowacki WK, Tobushi H (2006) Phase-Transformation Fronts Evolution for Stress- and Strain-Controlled Tension Tests in TiNi Shape Memory Alloy. Experimental Mechanics 46:531-542.
[12] Shaw JA and Kyriakides S (1997) On the nucleation and propagation of phase transformation fronts in NiTi alloy. Journal of the Mechanics and Physics of Solids 45(2):683-700.
[13] He YJ and Sun QP (2009) Scaling relationship on macroscopic helical domains in NiTi tubes. International Journal of Solids and Structures 46:4242-4251.
[14] Murasawa G, Yoneyama S, Sakuma T (2007) Nucleation, bifurcation and propagation of local deformation arising in NiTi shape memory alloy. Smart Materials and Structures 16:160-167.
[15] Adharapurapu RR, Jiang F, Vecchio KS, Gray III GT (2006) Response of NiTi shape memory alloy at high strain rate: A systematic investigation of temperature effects on tension-compression asymmetry. Acta Materialia 54:4609-4620.
[16] Chen W and Song B (2006) Temperature dependence of a NiTi shape memory alloy's superelastic behavior at high strain rate. Journal of Mechanics of Materials and Structures 1:339-356.
[17] Nemat-Nasser S and Choi JY (2005) Strain rate dependence of deformation mechanisms in a Ni-Ti-Cr shape-memory alloy. Acta Materialia 53:449-454.
[18] Nemat-Nasser S, Choi JY, GuoW-G, Isaacs JB (2005) Very high strain-rate response of a NiTi shape-memory alloy. Mechanics of Materials 37:287-298.
[19] Nemat-Nasser S and Guo W-G (2006) Superelastic and cyclic response of NiTi SMA at various strain rates and temperatures. Mechanics of Materials 38:463-474.
[20] Kolsky H (1949) An investigation of the mechanical properties of materials at very high strain

rates of loading. Proceedings of the Physical Society (London) 62-B:676-700.
[21] Zhao H and Gary G (1997) A new method for the separation of waves. Application to the SHPB technique for an unlimited duration of measurement. Journal of the Mechanics and Physics of Solids 45:1185-1202.
[22] Tobushi H, Shimeno Y, Hachisuka T, Tanaka K (1998) Influence of strain rate on superelastic properties of TiNi shape memory alloy. Mechanics of Materials 30:141-150.
[23] Qian L, Zhou Z, Sun QP, Yan W (2007) Nanofretting behaviors of NiTi shape memory alloy. Wear 63:501-507.
[24] Brinson LC, Schmidt I, Lammering R (2004) Stress-induced transformation behavior of a polycrystalline NiTi shape memory alloy: micro and macromechanical investigations via in situ optical microscopy. Journal of the Mechanics and Physics of Solids 52:1549-1571.
[25] Davies EDH and Hunter SC (1963) The dynamic compression testing of solids by the method of the split Hopkinson pressure bar. Journal of the Mechanics and Physics of Solids 11:55-179.
[26] Staab GH and Gilat A (1991) A direct-tension split Hopkinson bar for high strain rate testing. Experimental Mechanics 31(3):232-235.
[27] G.Gary, W.K.Nowacki, Essai de cisaillement plan appliqué à des tôle minces, Journal de physique Ⅳ. 4 (1994) C 8-65.
[28] J.R. Klepaczko, H. V. Nguyen, W.K. Nowacki, Quasi-static and dynamic shearing of sheet metals, J. Mech. A/solids. 18 (1999) 271-289.
[29] A. Rusinek, J.R. Klepaczko, Shear testing of a sheet steel at wide range of strain rates and a constitutive relation with strain-rate and temperature dependence of flow stress, International Journal of Plasticity. 17 (2001) 87-115.
[30] R. Merle, Mise en oeuvre et analyse d’un essai de double cisaillement en grandes déformations sous sollicitations dynamiques, France, 2003
[31] Hild F and Roux S (2006) Digital image correlation: from displacement measurement to identification of elastic properties, a review. Strain 42:69-80.
[32] Besnard G, Hild F, Roux S (2006) "Finite-element" displacement fields analysis from digital images: Application to Portevin-Le Chatelier bands. Experimental Mechanics 46(6):789-804.